ТЕХНІКА ТА МЕТОДИ ЕКСПЕРИМЕНТУ
ENGINEERING AND METHODS OF EXPERIMENT

УДК 615.849.1:539.172.3:519.245 https://doi.org/10.15407/jnpae2026.03.274

Bilalodin[1,*], F. Abdullatif[1], P. Lestari[2], S. Nurhayati[2], Zusfahair[2], Y. Sarjono[3], R. Tursinah[4]

[1] *Department of Physics, Faculty of Mathematics and Natural Sciences, Jenderal Soedirman University, Purwokerto, Indonesia*
[2] *Department of Chemistry, Faculty of Mathematics and Natural Sciences, Jenderal Soedirman University, Purwokerto, Indonesia*
[3] *Research Centre for Accelerator Technology, National Research and Innovation Agency, Jakarta, Indonesia*
[4] *Research Organization for Nuclear Energy, National Research and Innovation Agency, B. J. Habibie Science and Technology Park, Setu, Tangerang Selatan, Banten, Indonesia*

*Corresponding author: bilalodin@unsoed.ac.id

EFFECTIVENESS OF DOUBLE-LAYER BEAM SHAPING ASSEMBLY NEUTRON BEAM FOR BORON NEUTRON CAPTURE THERAPY: A MICRODOSIMETRIC STUDY USING PARTICLE AND HEAVY ION TRANSPORT CODE SYSTEM

Boron neutron capture therapy (BNCT) is a cancer therapy currently under development. The key to successful BNCT therapy depends on the ability of ^{10}B to be distributed within cells and the quality of the neutrons being used. The research aims to study the effectiveness of the neutron beam from Double-Layer Beam Shaping Assembly (DLBSA) in interacting with ^{10}B in producing α and ^{7}Li particles carried by two boron compounds: p-boronophenylalanine (BPA) and sodium borocaptate (BSH). The effectiveness of the neutron beam is evaluated using microdosimetric parameters by analyzing its range, linear energy transfer (LET) values, and dose distribution at the cellular level. The assessment was carried out using two cell geometry models, namely: single- and multi-cell. The neutron source comes from DLBSA with a neutron flux of $1.1\cdot10^{9}$ n/cm^2·s. The modeling, simulation, and calculation of microdosimetry parameters were carried out using the Particle and Heavy Ion Transport code System (PHITS) program. The study shows that the interaction between neutrons and ^{10}B produces α and ^{7}Li particles with ranges of 10 and 4 μm and LET values of 251.19 and 363.08 keV/μm. The dose distribution of α and ^{7}Li particles from the BPA compounds accumulates in the nucleus, and those from the BSH compounds in the cell membrane. Based on the microdosimetry study, neutron interactions from DLBSA can interact with ^{10}B using both the BPA and BSH compounds to produce α and ^{7}Li particles. The quality of the resulting α and ^{7}Li particles has met the therapeutic quality required in BNCT.

Keywords: boron neutron capture therapy, Double-Layer Beam Shaping Assembly, microdosimetry, alpha, lithium, linear energy transfer, dose.

1. Introduction

Boron neutron capture therapy (BNCT) is a cancer therapy method that utilizes thermal neutron irradiation on cancer cells previously injected with the boron isotope (^{10}B). The interaction of a neutron with ^{10}B produces ^{11}B, which spontaneously decays into ^{7}Li, producing an α particle and gamma radiation. The use of neutron reactions to treat tumors was introduced by Locher in 1936, which became the basis for the development of BNCT [1]. The first application of BNCT was performed in 1951 on a patient suffering from malignant glioma. The neutron source originates from the nuclear research reactor at the Brookhaven Graphite Research Reactor. The use of nuclear reactors as a neutron source faces several obstacles, which include strict security requirements, the presence of radiation waste from fission reactions, and very high installation costs [2]. Therefore, more environmentally friendly neutron sources were developed in the form of tandem accelerators and proton accelerators [3]. A proton accelerator produces fast neutrons using a Be or Li target [4].

One type of accelerator that is currently being developed is the cyclotron [5]. The neutrons generated by the cyclotron are not ready for use as a neutron source for BNCT because they are fast neutrons and the presence of numerous contaminants [6]. Therefore, a beam shaping assembly (BSA) is required to process the neutrons such that the output from the BSA acquires the characteristics of neutrons that satisfy the standard of the International Atomic Energy Agency (IAEA). The BSA consists of some components: moderator, reflector, collimator, and filter [7]. A Double-Layer Beam Shaping Assembly (DLBSA) design developed by Bilalodin et al. (2022) has effectively produced neutron beams that meet the IAEA standard. The resulting epithermal neutrons are more suitable for deeply located cancers [8].

A measurement of the penetrating power of neutrons from DLBSA has been carried out on a water phantom. The results showed that the neutron flux produced from DLBSA can penetrate the water phantom to a depth of 6 cm. The thermal neutron flux at this depth is $0.5\cdot10^{9}$ n/cm^2·s. It is at the minimum limit of neutron flux required in cancer therapy [9].

Apart from being studied for its penetrating power, the neutron beam from DLBSA has also been tested on several organs affected by cancer, including the head, thyroid, and lungs. The simulation results show that the neutron beam from DLBSA can produce the maximum dose to cure these cancers at a boron concentration of 60–70 ppm with an irradiation time of less than 1 h [10]. In this test, the distribution of boron is assumed to be spread throughout all parts of the tumor, notwithstanding that boron will be in the cell walls if the carrier compound is sodium boracaptate (BSH) and in the cell nucleus if the carrier compound is p-boronophenylalanine (BPA) [11]. Therefore, an effectiveness test of neutron radiation from DLBSA at the cellular level by considering the location of boron in cancer cells is required. The test on radiation at the cellular level is called a microdosimetry test [12].

This test is significant to determine the quality of the neutron radiation produced by DLBSA when it interacts with cancer cells. The results of the microdosimetry test will show the range of α and ^{7}Li particles, the linear energy transfer (LET) value, and the dose distribution in the cell components. Microdosimetry testing is also useful to determine the effective placement of ^{10}B in cancer cells, whether in the cell nucleus, cytoplasm, or cell wall. The effective placement is instrumental in the development of boron-carrier compounds.

Microdosimetry tests can be carried out using a Monte Carlo-based simulation approach. The Monte Carlo method is an excellent technique to understand the mechanisms of radiation effects at the cellular level [13]. One of the Monte Carlo-based software programs currently being developed is the Particle and Heavy Ion Transport code System (PHITS). This software has been successfully developed to support medical research [14]. In this research, evaluation of neutron beam effectiveness will be carried out on neutron beams produced by the DLBSA system on single-cell and multi-cell cells for the development of BNCT therapy.

2. Materials and methodology

2.1. Model of cell and its composition

Microdosimetric analyses of neutron beams from the DLBSA were performed using both single-cell and multicellular models. Single-cell and multi-cell models are composed of the cell nucleus, cytoplasm A, cytoplasm B, and the cell membrane with radii of 1, 2, 4, and 5 μm, respectively. Meanwhile, the multi-cell model consists of seven closely packed cells [15]. Fig. 1 shows the single-cell and multi-cell models.

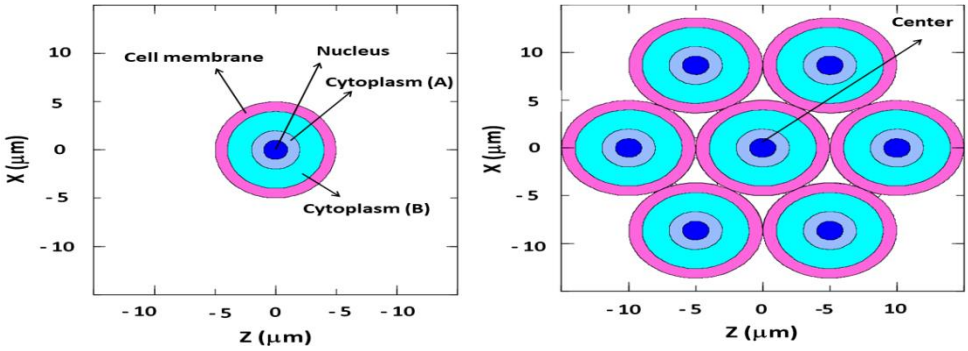

a *b*

Fig. 1. Models of cancer cells: *a* – single-cell model; *b* – multi-cell model.
(See color Figure on the journal website.)

Cancer cells are composed of the elements hydrogen, carbon, nitrogen, oxygen, and phosphorus, which refer to International Commission on Radiation Units and Measurements Report 44 [16]. The placement of ^{10}B is based on the characteristics of the boron-bearing compound. The boron-bearing compound BSH accumulates in the cell membrane, and the boron-bearing compound BPA accumulates in the cell nucleus. The boron concentration used is 70 ppm.

2.2. Limitations of the model

In this study, single-cell and multi-cell models are utilized to investigate the microdosimetric characteristics of α particles and ^{7}Li ions resulting from ^{10}B(n,α)^{7}Li reactions. The underlying geometry is simplified to maintain computational efficiency while facilitating the evaluation of fundamental neutron-boron interactions and energy deposition mechanisms at the cellular level. In this framework, the single-cell model is represented as a sphere comprising a cell membrane, cytoplasm, and nucleus. Furthermore, the multi-cell model consists of a periodic lattice of identical cells characterized by uniform dimensions and intercellular distances. This geometric simplification does not capture the morphological heterogeneity and spatial distribution of actual cells and tissues. Hence, the proposed model serves as a theoretical approximation aiming to evaluate broad microdosimetric

trends rather than providing an exact representation of biological responses.

Another essential assumption pertains to the cellular distribution of boron. The concentration of boron, carried by BPA and BSH, is assumed to be distributed homogeneously in the designated areas. In reality, boron absorption is influenced by cell metabolism, transport mechanisms, and tissue heterogeneity, resulting in a heterogeneous distribution both intercellularly and in subcellular structures [17]. Consequently, the dose distribution obtained from the simulation may differ from the dose distribution in actual biological tissues.

Additionally, the model does not account for complex biological factors, such as variations in cellular radiosensitivity, deoxyribonucleic acid (DNA) repair mechanisms, cell cycle, or the tumor microenvironment. Instead, this work focuses particularly on physical aspects of energy depositions resulting from neutron capture reactions.

2.3. Neutron source

The neutron source originates from a 30 MeV cyclotron, processed using a DLBSA system. The neutrons produced from DLBSA have characteristics of an epithermal neutron flux of $1.1 \cdot 10^9$ n/cm^2·s, a ratio of epithermal neutron flux and thermal neutron flux of 344, a ratio of epithermal neutron flux and fast neutron flux of 85, a ratio of fast neutron dose rate and the epithermal flux is $1.09 \cdot 10^{-13}$ Gy·cm^2, and the comparison of gamma dose rate and epithermal neutron flux is $1.82 \cdot 10^{-13}$ Gy·cm^2 [18].

2.4. Determination of microdosimetry parameters

The neutron beam required in BNCT therapy is neutrons that can interact with ^{10}B and produce α and ^{7}Li particles. Calculation of the range of α and ^{7}Li particles, LET, and dose distribution in cells utilizes PHITS software developed by the Japanese Atomic Energy Agency. The data library used is JENDL-40. The parameters were determined using 10 million particles. Determination of the range and footprint of α and ^{7}Li particles uses the track tally, linear energy transfer uses the LET tally, and dose distribution uses the deposit tally [19].

3. Results and discussions

When neutrons from the DLBSA irradiate a cell that contains boron (^{10}B), the thermal neutrons will react with ^{10}B and form ^{11}B. The ^{11}B isotope decays to produce α and ^{7}Li particles. The mechanism for the formation of α and ^{7}Li particles occurs in two ways. First, the interaction of neutrons with ^{10}B produces α particles with an energy of 1.78 MeV and ^{7}Li with an energy of 1.01 MeV. Both produce α and ^{7}Li particles in an excited state. The ^{7}Li ion then decays to the ground state while emitting gamma rays with an energy of 0.428 MeV, α particles (1.47 MeV), and ^{7}Li (0.84 MeV). The percentage of occurrence of the first mechanism is 6.3 %, and the second mechanism is 93.7 % [20].

3.1. The range of α and ^{7}Li particles

The interaction of thermal neutrons with ^{10}B atoms produces α and lithium ^{7}Li particles in the cell. The range of α and ^{7}Li particles is relatively short, namely in the order of micrometers. The range of α particles is about 9 μm, and ^{7}Li is about 4 μm. This finding aligns with the research results of Pitto–Barry (2021), which states that the range of α and ^{7}Li particles is around 4–9 μm [21]. Such characteristics of a range of α and ^{7}Li particles can potentially damage the DNA of cancer cells. Optimal cell damage by α and ^{7}Li particles occurs when interactions between thermal neutrons and ^{10}B in the cell reach the value of 10^9 atoms/cell or 20 μg/g [22]. The range of α and ^{7}Li particles in the cell is shown in Fig. 2.

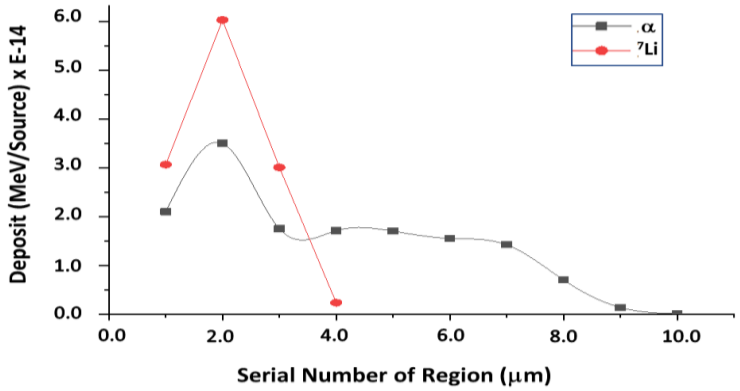

Fig. 2. The range of α and ^{7}Li particles. (See color Figure on the journal website.)

The difference in range between α and ^{7}Li particles is likely due to the difference in kinetic energy at the time of their formation. The kinetic energy of α and ^{7}Li particles in the first formation reaction (6.3 %) is 1.47

and 0.84 MeV. In the second formation mechanism (93.7 %), the α and ^{7}Li particles produce higher kinetic energy, namely 1.78 and 1.01 MeV [23].

3.2. LET

LET is the average energy transferred through a medium per unit length. The unit for the LET value is kiloelectronvolts per micrometer (keV/μm). The simulation results of the LET values of α and ^{7}Li particles show that the lowest LET value for α particles is 33 keV/μm and the highest is 251.19 keV/μm. Meanwhile, the obtained LET values of ^{7}Li are 70 keV/μm at the lowest and 363.08 keV/μm at the highest. The results of the LET α and ^{7}Li values disagree with the research results of Hu et al. (2020) and Mukawa et al. (2011) [24, 25]. The disagreement results from the difference in neutron flux and concentration of ^{10}B used in the respective calculations. According to Conte et al. (2023), the LET resulting from the interaction of thermal neutrons with ^{10}B is influenced by the amount of boron [26]. The LET values of α and ^{7}Li particles are shown in Fig. 3.

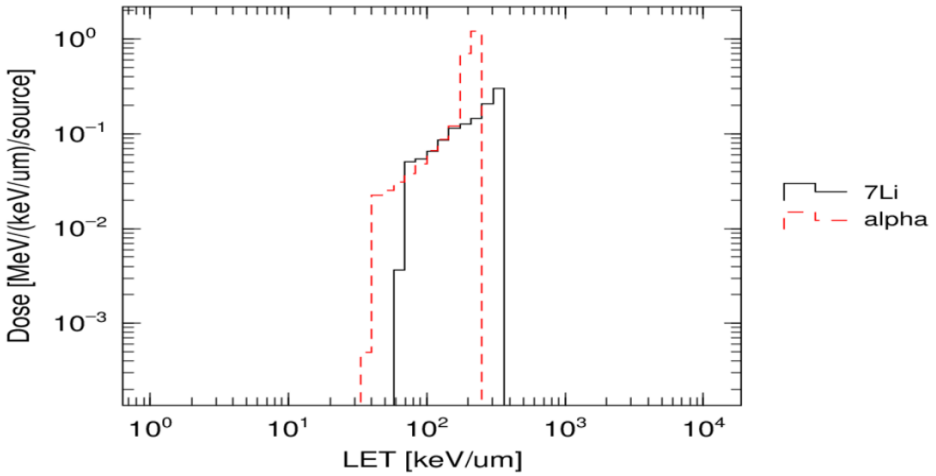

Fig. 3. LET value of α and ^{7}Li particles. (See color Figure on the journal website.)

3.3. Determination of dose distribution

Determination of dose distribution in single and multi cells is carried out using the deposit tally. The determination is conducted in the cell nucleus, cytoplasm A, cytoplasm B, and the cell membrane. The dose distribution being determined is the boron dose, consisting of α and ^{7}Li doses. The boron dose contributes the highest (85 %) in the calculation of the BNCT dose [27].

Distribution in a single-cell model. The simulation results of the particle-trace distribution of α and ^{7}Li in a single-cell model using the compound BPA are shown in Fig. 4. The figure shows that the highest intensity of α and ^{7}Li particles occurs in the cell nucleus and decreases in the cytoplasm and cell walls. Traces of α and ^{7}Li particles also penetrate out of the cell with low intensity. Such high intensity of α and ^{7}Li particles is due to the BPA compound being able to penetrate the cell wall so that boron can accumulate in the cell nucleus [28].

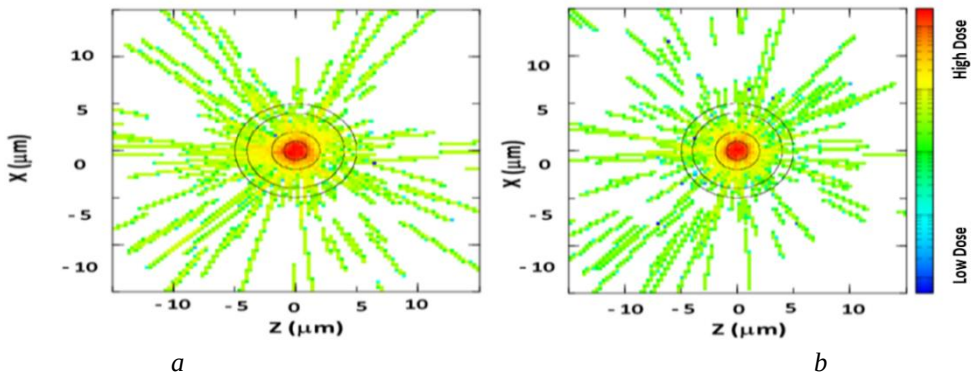

a *b*

Fig. 4. Visualization of the dose distribution of α and ^{7}Li particles in a single cell using the BPA compound: *a* – α particle, *b* – ^{7}Li particle. (See color Figure on the journal website.)

The results of the particle tracing test in a single cell using the boron-carrier compound BSH are shown in Fig. 5. The figure shows that the intensity of α and ^{7}Li particles is highest in the cell membrane. The distribution of α and ^{7}Li particles also spreads into the cell nucleus and outside the cell wall with low

intensity. The highest intensity of α and ^{7}Li particles only occurs in the cell wall because BSH is a boron-carrying compound with low transport selectivity, which can deliver boron only to the cell wall [29].

Complete data of dose distribution values in single and multi cells using the boron-carrier compounds BPA and BSH are shown in Table 1. The table shows that the dose of α and ^{7}Li particles using the boron-carrier compound BPA produces a high dose value of 17.8 Gy in the cell nucleus. Meanwhile, the dose of α and ^{7}Li particles in the single-cell model using the BSH boron-carrier compound produced a high dose value of 8.79 Gy on the cell membrane. This result shows that the BPA boron carrier is more effective than the BSH boron-carrier compound.

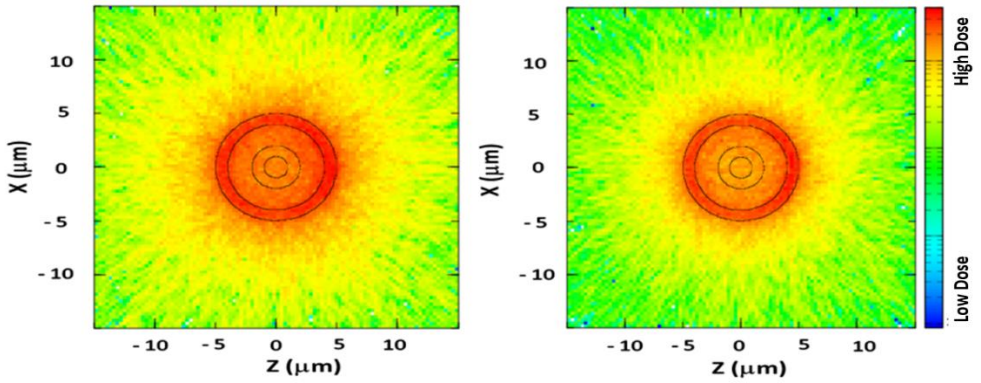

a *b*

Fig. 5. Visualization of the dose distribution of α and ^{7}Li particles in a single cell using the BSH compound: *a* – α particle, *b* – ^{7}Li particle. (See color Figure on the journal website.)

Table 1. **The dose of α and ^{7}Li particles in the single-cell model using the BPA and BSH compounds**

Boron-carrying compound	Area	Cell nucleus, Gy	Cytoplasm A, Gy	Cytoplasm B, Gy	Cell membrane, Gy
BPA	α	6.50	1.32	0.30	0.07
	^{7}Li	11.30	2.19	0.50	0.02
	Total	17.80	3.51	0.80	0.08
BSH	α	0.03	0.02	2.14	3.11
	^{7}Li	0.05	0.04	3.72	5.68
	Total	0.08	0.06	5.86	8.79

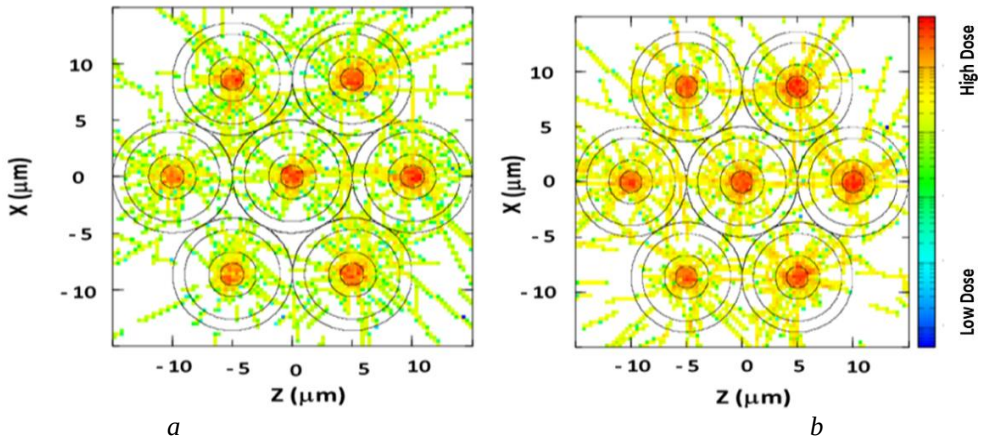

a *b*

Fig. 6. Distribution of dose in a multi-cell model for the BPA compound: *a* – α particle, *b* – ^{7}Li particle. (See color Figure on the journal website.)

Distribution in the multi-cell model. Fig. 6 shows the traces of α and ^{7}Li particles in the multi-cell model using the BPA compounds. The figure shows that the highest intensity of α and ^{7}Li particles occurs in the cell nucleus and decreases in the cytoplasm and cell wall. Traces of α and ^{7}Li particles also affect the surrounding cells with very low intensity. Such dominant traces of α and ^{7}Li particles in cells suggest that BNCT is a targeted cell-based therapy. Such therapy is safe for neighboring healthy cells [30].

Dose distribution characteristics of α and ^{7}Li particles are different when the BSH boron-carrier com-

pound is used. The dose distribution of α and ^{7}Li particles with the BSH boron-carrier compound accumulates in cell membranes. The dose also spreads into the cell nucleus and outside the cell wall. The maximum intensity of α and ^{7}Li particles occurs at the cell membrane. This is due to the low selectivity of the BSH compound, causing it to be able to enter the cell wall [31]. The traces of the α and ^{7}Li particles in the multi-cell model using the BSH compound are shown in Fig. 7.

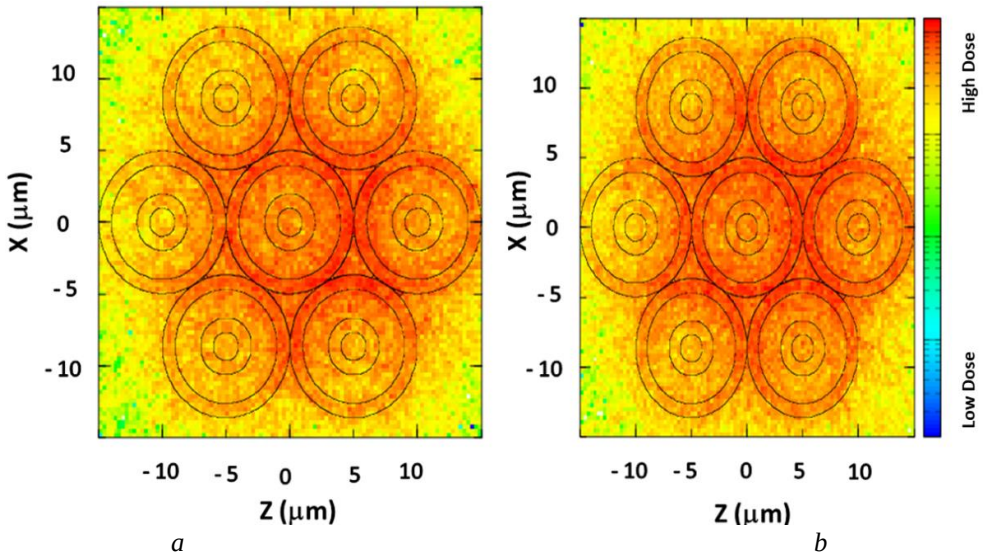

a *b*

Fig. 7. Distribution of dose in a multicell model for the BSH compound: *a* – α particle, *b* – ^{7}Li particle. (See color Figure on the journal website.)

Table 2. **Dose of α and ^{7}Li particles in the multi-cell model using the BPA and BSH compounds**

Boron-carrying compound	Area	Cell nucleus, Gy	Cytoplasm A, Gy	Cytoplasm B, Gy	Cell membrane, Gy
BPA	α	1.75	0.38	0.14	0.05
	^{7}Li	3.42	0.64	0.20	0.09
	Total	5.17	1.02	0.34	0.14
BSH	α	0.01	0.07	0.65	0.88
	^{7}Li	0.02	0.12	1.14	1.60
	Total	0.03	0.19	1.79	2.48

The dose distribution values for each component in the single- and multi-cell models using the boron-carrier compounds BPA and BSH are shown in Table 2. The table shows that the dose values for α and ^{7}Li particles in the cell nucleus are 5.17 Gy using the BPA compound and 2.48 Gy on cell walls using the BSH compound. The dose values for α and ^{7}Li using BPA are higher than with BSH because the use of BSH causes a significant number of α and ^{7}Li particles to spread out of the cell nucleus.

The results of microdosimetry findings in this study are subject to some uncertainties inherent in the Monte Carlo simulation method [32]. First, statistical uncertainty arises from the finite number of simulated particle histories; consequently, the computed dose values represent estimates bounded by a specific variance. Second, the structural model employs a simplified representation of actual biological morphology. While this geometric abstraction significantly enhances computational efficiency, it fails to fully capture the complex cellular architecture and organelle distributions that influence energy deposition at the microscopic level. Finally, systemic uncertainty stems from the assumption of a homogeneous boron distribution across the entire cellular volume, whereas, in reality, boron localization is highly heterogeneous at both the cellular and subcellular levels.

Despite the uncertainties arising from various origins, the utilized model can provide quantitative descriptions of dose deposition characteristics and microdosimetric responses of various irradiation scenarios. Consequently, the findings are better suited to evaluate trends and relative comparisons among simulation scenarios rather than being an absolute representation of real biological conditions. Future work should consider the development of more realistic cell geometry, heterogeneous boron distribution, and integration of experimental radiobiological data to enhance the accuracy and validity of BNCT dosimetry.

4. Conclusions and suggestions

Analysis of neutron beams generated by the DLBSA reveals that the range of α and ^{7}Li particles resulting from ^{10}B(n,α)^{7}Li are approximately 9 μm and 4 μm, respectively, with corresponding LET values of 251.19 keV/μm and 363.08 keV/μm. In the single-cell model, the maximum dose delivered via BPA reaches 17.9 Gy within the nucleus, whereas BSH yields 8.79 Gy at the cell membrane. In the multicell model, the maximum dose is 5.17 Gy in the nucleus and 2.48 Gy at the wall for BSH. The findings demonstrate that BPA induces a higher deposition dose than BSH, due to its superior target-cell selectivity. The similar characteristics of dose distribution in single-cell and multi-cell models highlight the consistency of microdosimetric responses under neutron irradiation from the DLBSA system. Overall, the findings of this study underscore the promising potential of DLBSA neutron beam for BNCT applications. This work is a preliminary evaluation based on simulations with simplified cell geometries assuming homogeneous boron distribution. Therefore, further studies employing more realistic biological models and experimental validations are required to comprehensively evaluate the adequacy of DLBSA as a neutron source for BNCT.

REFERENCES

1. K. Nedunchezhian et al. Boron neutron capture therapy – A literature review. J. Clin. Diagn. Res. 10(12) (2016) ZE01.
2. A.M. Dymova et al. Boron neutron capture therapy: Current status and future perspectives. Cancer Commun. 40(9) (2020) 406.
3. I.S. Anderson et al. Research opportunities with compact accelerator-driven neutron sources. Phys. Rep. 654 (2016) 1.
4. Yi-Nan Zhu et al. Study on the optimal incident proton energy of ^{7}Li(p, n)^{7}Be neutron source for boron neutron capture therapy. Nucl. Sci. Tech. 35(3) (2024) 60.
5. Y. Matsumoto et al. A critical review of radiation therapy: From particle beam therapy (proton, carbon, and BNCT) to beyond. J. Pers. Med. 11(8) (2021) 825.
6. X. Zhang, Y. Lin. Developments in neutron sources for boron neutron capture therapy. In: Y. Zhu (Ed.). Frontiers in Boron-Based Medicinal Chemistry. Chapter 5 (Singapore: World Scientific, 2023) p. 115.
7. G. Li et al. Design of beam shaping assemblies for accelerator-based BNCT with multi-terminals. Front. Public Health 9 (2021) 642561.
8. Bilalodin et al. Optimization and verification of double layer beam shaping assembly (DLBSA) for epithermal neutron generation. J. Teknol. 84(4) (2022) 103.
9. Bilalodin et al. The testing of epithermal neutron beams produced by the double layer beam shaping assembly (DLSBA) on a water phantom using particle heavy ion transport system (PHITS). Proceeding ICMA-SURE 3(1) (2024) 209.
10. Bilalodin et al. Dosimetry analysis of boron neutron capture therapy (BNCT) on thyroid cancer using PHITS code with neutron from 30 MeV cyclotron. J. Teknol. 85(5) (2023) 21.
11. F.R. Barth, P. Mi, W. Yang. Boron delivery agents for neutron capture therapy of cancer. Cancer Commun. 38 (2018) 35.
12. J. Vohradsky et al. Evaluation of silicon based microdosimetry for Boron Neutron Capture Therapy Quality Assurance. Phys. Med.: Eur. J. Med. Phys. 66 (2019) 8.
13. P. Shamshiri, G. Forozani, A. Zabihi. An investigation of the physics mechanism based on DNA damage produced by protons and alpha particles in a realistic DNA model. Nucl. Instrum. Methods B 454 (2019) 40.
14. T. Furuta, T. Sato. Medical application of particle and heavy ion transport code system PHITS. Radiol. Phys. Technol. 14(3) (2021) 215.
15. A. Karaoglu et al. Calculation by GAMOS/Geant4 simulation of cellular energy distributions from alpha and lithium-7 particles created by BNCT. Appl. Radiat. Isot. 132 (2018) 206.
16. P. Qi et al. The potential role of borophene as a radiosensitizer in boron neutron capture therapy (BNCT) and particle therapy (PT). Biomater. Sci. 8(10) (2020) 2778.
17. B. Marcaccio et al. Unraveling the role of boron microdistribution in BNCT dosimetry of glioblastoma multiforme: combined theoretical and experimental insights. Phys. Med. Biol. 71(8) (2026) 085004.
18. Bilalodin et al. Microdosimetry test on double layer beam shaping assembly neutron beam as a boron neutron capture therapy neutron source using PHITS code. Nucl. Phys. At. Energy 25(4) (2024) 388.
19. T. Sato et al. Features of particle and heavy ion transport code system (PHITS) version 3.02. J. Nucl. Sci. Technol. 55(6) (2018) 684.
20. L. Moghaddasi, E. Bezak. Geant4 beam model for boron neutron capture therapy: investigation of neutron dose components. Australas. Phys. Eng. Sci. Med. 41(1) (2018) 129.
21. A. Pitto-Barry. Polymers and boron neutron capture therapy (BNCT): a potent combination. Polym. Chem. 12(14) (2021) 2035.
22. S.-I. Miyatake et al. Boron neutron capture therapy for malignant brain tumors. Neurol. Med. Chir. 56(7) 2016) 361.
23. H. Fukunaga. Implications of radiation microdosimetry for accelerator-based boron neutron capture therapy: a radiobiological perspective. Br. J. Radiol. 93(1111) (2020) 20200311.
24. N. Hu et al. Evaluation of PHITS for microdosimetry in BNCT to support radiobiological research. Appl. Radiat. Isot. 161 (2020) 109148.
25. T. Mukawa, T. Matsumoto, K. Niita. Study on microdosimetry for boron neutron capture therapy. Prog. Nucl. Sci. Technol. 2 (2011) 242.

26. V. Conte, A. Bianchi, A. Selva. Boron neutron capture therapy: Microdosimetry at different boron concentrations. Appl. Sci. 14(1) (2024) 216.
27. Y.-C. Teng et al. Correcting for the heterogeneous boron distribution in a tumor for BNCT dose calculation. Sci. Rep. 13(1) (2023) 15741.
28. M. Lamba, A. Goswami, A. Bandyopadhyay. A periodic development of BPA and BSH based derivatives in boron neutron capture therapy (BNCT). Chem. Commun. 57(7) (2021) 827.
29. H. Xu et al. Novel promising boron agents for boron neutron capture therapy: Current status and outlook on the future. Coord. Chem. Rev. 511 (2024) 215795.
30. T. Tani et al. Advanced boron neutron capture therapy targeting cancer stem cells by selective induction of LAT1 overexpression. Radiat. Res. 200(1) (2023) 21.
31. D.S. Seneviratne et al. Next-generation boron drugs and rational translational studies driving the revival of BNCT. Cells 12(10) (2023) 1398.
32. B. Zhao et al. Research on hybrid methods for variance reduction in Monte Carlo dose calculation of BNCT. Nucl. Eng. Technol. 58 (2026) 104254.

Білалодін[1,*], Ф. Абдуллатіф[1], П. Лестарі[2], С. Нурхаяті[2], Зусфахаір[2], Ю. Сарджоно[3], Р. Турсінах[4]

[1] Кафедра фізики, факультет математики та природничих наук, Університет Джендерела Судірмана, Пурвокерто, Індонезія
[2] Кафедра хімії, факультет математики та природничих наук, Університет Джендерела Судірмана, Пурвокерто, Індонезія
[3] Дослідницький центр технологій прискорювачів, Національне агентство досліджень та інновацій, Джакарта, Індонезія
[4] Дослідницька організація з ядерної енергетики, Національне агентство досліджень та інновацій, Науково-технологічний парк ім. Б. Дж. Хабібі, Сету, Південний Тангеранг, Бантен, Індонезія

*Відповідальний автор: bilalodin@unsoed.ac.id

ЕФЕКТИВНІСТЬ ДВОШАРОВОЇ СИСТЕМИ ФОРМУВАННЯ НЕЙТРОННОГО ПУЧКА ДЛЯ БОР-НЕЙТРОН-ЗАХОПЛЮВАЛЬНОЇ ТЕРАПІЇ: МІКРОДОЗИМЕТРИЧНЕ ДОСЛІДЖЕННЯ З ВИКОРИСТАННЯМ ПРОГРАМНОГО КОМПЛЕКСУ ДЛЯ МОДЕЛЮВАННЯ ПЕРЕНОСУ ЧАСТИНОК І ВАЖКИХ ІОНІВ

Бор-нейтрон-захоплювальна терапія (BNCT) – це метод лікування раку, що наразі перебуває на стадії розробки. Успіх BNCT залежить від здатності ізотопу ^{10}B розподілятися всередині клітин та від якості використовуваних нейтронів. Метою дослідження є оцінка ефективності нейтронного пучка, сформованого двошаровою системою (DLBSA), у взаємодії з ^{10}B для утворення α-частинок та ^{7}Li за участю двох сполук бору: р-боронофенілаланіну (BPA) та натрію борокаптату (BSH). Ефективність пучка оцінювали за допомогою мікродозиметричних параметрів: аналізу пробігу частинок, значень лінійної передачі енергії (ЛПЕ) та розподілу дози на клітинному рівні. Оцінку проводили з використанням двох геометричних моделей клітин: одноклітинної та багатоклітинної. Джерелом нейтронів була система DLBSA з потоком нейтронів $1{,}1\cdot10^{9}$ н/(см^2·с). Моделювання та розрахунок мікродозиметричних параметрів здійснювали за допомогою програмного комплексу PHITS (Particle and Heavy Ion Transport code System). Результати дослідження свідчать, що внаслідок взаємодії нейтронів із ^{10}B утворюються α-частинки та ^{7}Li з пробігом 10 і 4 мкм та значеннями ЛПЕ 251,19 і 363,08 кеВ/мкм відповідно. Розподіл дози від α-частинок та ^{7}Li, утворених зі сполук BPA, характеризується накопиченням у ядрі клітини, тоді як у випадку сполук BSH – у клітинній мембрані. Мікродозиметричне дослідження підтвердило, що нейтрони від системи DLBSA можуть взаємодіяти з ^{10}B (у складі сполук BPA або BSH) з утворенням α-частинок та ^{7}Li. Характеристики отриманих α-частинок та ^{7}Li відповідають вимогам до якості випромінювання, необхідним для BNCT.

Ключові слова: бор-нейтрон-захоплювальна терапія, двошарова система формування пучка (DLBSA), мікродозиметрія, α-частинки, літій, лінійна передача енергії, доза.

Надійшла / Received 05.08.2025